

Continuum Sensitivity Method for Aeroelastic Shape Design Problems *

Shaobin Liu[†] and Robert A. Canfield[‡]

Virginia Tech, Blacksburg, VA, 24061, USA

A Continuum Sensitivity Equation (CSE) method is developed for transient nonlinear aeroelastic problems. The continuum sensitivity equations and sensitivity boundary conditions are derived for a built-up joined beam structure under transient aerodynamic loads which are obtained by solving the potential flow equations. The pseudo solid method is adopted for both mesh movement and design velocity calculation. For built-up structures with strain discontinuity at the joints, the total form CSE is easier to implement than the local form. In this paper, a coupled fluid-structure physics and continuum sensitivity equations for gust response of a nonlinear joined beam with an airfoil model are posed and solved. The results are compared to the results obtained by finite difference (FD) method.

I. Introduction

IN the continuum sensitivity method, also known as variational shape design,¹ the continuous sensitivity equation method,² and the variational sensitivity method,³ the design parameter gradients are calculated by solving the continuum sensitivity equations, typically a system of linear partial differential equations. The sensitivity system is always a linear system of equations, even when the original system is nonlinear. If Newton-Raphson iteration is used for the nonlinear problems, the tangent stiffness matrix of the last iteration gives the sensitivity matrix for the linear system of CSE equations, as previous researchers, Borggaard,⁴ Wickert,⁵ Liu and Canfield,⁶ have noted.

The continuum sensitivity methods were first introduced for structural problems.^{7,8} Jameson first introduced continuum sensitivity concept in adjoint equation form for aerodynamic design problems.⁹ The landmark Borggaard and Burns paper⁴ introduced the CSE nomenclature in a fluid setting and several fluid flow optimization applications followed.^{2,10-12} Choi¹³ cites the lion's share of structural elasticity applications that employ continuum sensitivity methods. Bhaskaran and Berkooz¹⁰ present one of the earliest continuum sensitivity solution for fluid-structure interaction problem, but limited to one-way coupling from structure to fluid. Pelletier et al. have employed continuum sensitivity methods for a range of fluid-structure interaction problems¹⁴⁻¹⁶ with prominent success. Their work focuses primarily on flow variable sensitivities. Wickert and Canfield applied the CSE method to the gust sensitivity for simple airfoil mounted to a 1D Euler Bernoulli Beam.¹⁷ Recent work¹⁸ has applied the CSE method to built-up structures for static aeroelastic cases. The current effort extends this method to a transient nonlinear joined beam with an airfoil using Garlerkin finite element method. Newton-Raphson iteration is used for the nonlinear problem and for obtaining the coefficient matrix for the linear CSE. Boundary conditions are also derived for CSE of the built-up structure sensitivity problems.

Continuum sensitivity systems are often posed in terms of local derivatives (an Eulerian reference frame), although it is possible to derive the CSE system in total derivative form (Lagrangian reference frame).¹⁹ For shape optimization of fluid applications, an Eulerian description of the flow sensitivity is usually adequate.

*The views and conclusions contained herein are those of the authors and should not be interpreted as necessarily representing the official policies or endorsements, either expressed or implied, of Air Force Office of Scientific Research or the U.S. Government. The U.S. Government is authorized to reproduce and distribute reprints for Governmental purposes notwithstanding any copyright notation thereon.

[†]Ph.D. Candidate, Department of Aerospace and Ocean Engineering, Virginia Tech, 214 Randolph Hall, Blacksburg VA, 24061, AIAA Member.

[‡]Professor, Department of Aerospace and Ocean Engineering, Virginia Tech, 214 Randolph Hall, Blacksburg VA, 24061, AIAA Associate Fellow

Thus, much of the fluid mechanics literature does not emphasize the distinction between the local and total derivative. For structural optimization problems, however, the design sensitivity at a material point is usually required, which necessitates a means to calculate total sensitivities at a given material point. Wickert and Canfield¹⁷ compute local derivatives and convert to total derivatives. In this work, the total form continuum sensitivity method for calculating the total sensitivity directly is investigated and compared with the local form. The advantages of total form CSE for shape sensitivity problems, especially for built-up structures, are discussed.

Section II derives the continuum sensitivity system and its associated boundary conditions. The next section gives the equations and boundary conditions for solving a simple fluid-structure model for a joined beam structure. The CSE and its boundary conditions for both structure and fluid domain are derived in details. This example is fairly simple, yet complex enough to capture all the salient aspects of a continuum sensitivity calculation for a coupled domain, nonlinear, transient system. It demonstrates the advantages of the total form CSE for built-up structure problems. This is followed by a brief description of the computational results. The results are compared with the finite difference calculations.

II. Continuum Sensitivity Equations

Consider the following general, nonlinear boundary value system defined in a domain Ω with a boundary Γ for which we seek a solution $u(x, t; b)$ of the equations

$$A(u, L(u)) = f(x, t; b) \quad \text{on } \Omega \quad (1)$$

with geometric and natural boundary conditions

$$B(u, L(u)) = g(x, t; b) \quad \text{on } \Gamma \quad (2)$$

where $u = u(x, t; b)$ is dependent on design variable b implicitly, $L(u)$ is a vector of linear differential operators, such as $\left\{ \frac{\partial}{\partial t}, \frac{\partial}{\partial x}, \frac{\partial}{\partial y}, \frac{\partial^2}{\partial x^2}, \frac{\partial^2}{\partial y^2}, \dots \right\}$, that appears in the governing differential equations or boundary conditions, A and B are vectors of algebraic functions of u and $L(u)$, and $B(u, L(u))$ can be a simple function of u , such as a prescribed boundary condition $u = \bar{u}$ for Dirichlet boundary conditions, or involve a differential operator for von Neumann boundary conditions.

Discrete sensitivity analysis methods discretize the original governing equations (1) and obtain a system of discrete equations first. For example, in the static case

$$\mathbf{K}\mathbf{u} = \mathbf{f} \quad (3)$$

Then, the sensitivity with respect to the design parameters, $\frac{D\mathbf{u}}{Db}$, can be calculated by using the finite difference method or discrete analytical methods.

The total derivative of solution vector \mathbf{u} with respect to design parameter b is $\frac{D\mathbf{u}}{Db}$. The finite difference method can be used for approximating $\frac{D\mathbf{u}}{Db}$. For example, the forward difference approximation is

$$\frac{D\mathbf{u}}{Db} \simeq \frac{\mathbf{u}(b + \Delta b) - \mathbf{u}(b)}{\Delta b} \quad (4)$$

A drawback of the finite difference method is the challenge of determining the optimum step size. Large step sizes are dominated by truncation error and small step sizes are dominated by numerical round-off error. Furthermore, it involves solving the original analysis problem $n+1$ times for n design variables, which makes finite difference method inefficient, especially for nonlinear problems.

Discrete analytical methods require the derivatives of the stiffness matrix and load vectors with respect to the design variables. The direct method differentiates Eq. (3) and solves for

$$\frac{D\mathbf{u}}{Db} = \mathbf{K}^{-1} \left(\frac{D\mathbf{f}}{Db} - \frac{D\mathbf{K}}{Db} \mathbf{u} \right) \quad (5)$$

where \mathbf{K} is the stiffness matrix of the discretized equation of Eq. (1). If the design parameter is a shape parameter, the mesh sensitivity in the whole domain should be calculated for $\frac{D\mathbf{K}}{Db}$, which is computationally inefficient.

The CSE method avoids these shortcomings by directly differentiating the governing equation. Taking the partial derivative of the governing equations (1), the CSEs can be obtained in terms of local sensitivity variable $u' = \frac{\partial u}{\partial b}$ as

$$\frac{\partial A}{\partial u} u' + \frac{\partial A}{\partial L} L(u') = \frac{\partial f(x, t; b)}{\partial b} \quad (6)$$

Their boundary conditions may be derived by taking material derivative of the boundary condition (2) and writing the material derivatives in terms of local derivatives and convective terms as

$$\frac{Du}{Db} = \frac{\partial u}{\partial b} + V(x) \cdot \nabla u \quad (7)$$

where ∇u is the gradient of u with respect to the spatial coordinates, $V(x) = \frac{\partial X}{\partial b}$ is the geometric sensitivity or design velocity, which is dependent on the parameterization of the computational domain. $X = x + bV(x)$ is the coordinates of a material point. After taking material derivatives of (2) and moving the convective terms to the right hand side, the CSE boundary conditions are given as

$$\frac{\partial B}{\partial u} u' + \frac{\partial B}{\partial L} L(u') = \dot{g}(x, t; b) - V(x) \cdot \left(\frac{\partial B}{\partial u} \nabla u + \frac{\partial B}{\partial L} L(\nabla u) \right) \quad (8)$$

where $\dot{g}(x, t; b)$ is the material derivative of the boundary condition which is 0 when g is not dependent on the design. The commutation of derivatives on the left side of Eq. (8) is possible when the derivatives are local. The CSE, Eq. (6), with the boundary conditions in Eq. (8) is a well posed linear system of equations in terms of sensitivity variable u' , which can be solved by the same numerical method used for solving the analysis problem. The solution u can be obtained from the analysis solution of Eq. (1) for use in Eq. (6) and Eq. (8). The CSE in local form only requires the design velocity, $V(x)$, at the boundaries. The boundary velocity method is more efficient when only sensitivities at boundaries are of interest, since it avoids calculating design velocity inside the whole domain.

The solution of CSE (7)-(8) is local sensitivity. The total derivative of u with respect to design parameter b at a material point consists of the local derivative and the convective term. The latter accounts for how u changes as the material point moves in response to design variable changes. After solving for the local derivative, the total derivative can be obtained by using Eq. (7).

Another way to calculate the material derivatives is to form the CSE equations in terms of total sensitivity variable, $\dot{u} = \frac{Du}{Db}$ and solve these equations directly without conversion. The total derivative form CSE equations are derived by taking material derivatives of the governing equations or the weak form of the governing equations. Suppose state variable $u(x)$ is smooth, and the design parameterization is defined such that the deformation mapping is linear, namely

$$X = x + bV(x)$$

where $V(x)$ is the design velocity. The material derivative of a state variable in Eq. (7) can be written as

$$\dot{u} = u'(x) + V(x) \cdot \nabla u \quad (9)$$

The material derivative of a domain functional may be used for deriving the CSE equations. Let ψ be a domain functional, defined as an integral over Ω , namely,

$$\psi = \int_{\Omega} f(x) d\Omega$$

where $f(x)$ is a function defined in Ω . The material derivative of ψ at Ω is

$$\dot{\psi} = \int_{\Omega} [f'(x) + \operatorname{div}(fV)] d\Omega \quad (10)$$

For deriving the total form CSE, firstly, we derive the weak form for the governing equations Eq. (1) and write it as

$$\int_{\Omega} C(w, \bar{w}) d\Omega = \int_{\Omega} \bar{w}^T f d\Omega$$

where $C(w, \bar{w})$ is the integrand of the weak form and \bar{w} is the test function. Taking the total derivative of the weak form with respect the design variable by using Eq. (9) and Eq. (10), we have

$$\int_{\Omega} [C(w, \dot{\bar{w}} - \nabla \bar{w} V) + C(\dot{w} - \nabla w V, \bar{w})] + \operatorname{div}(C(w, \bar{w}) V) d\Omega = \int_{\Omega} (\dot{\bar{w}} - \nabla \bar{w} V)^T f + \dot{f} \bar{w} d\Omega \quad (11)$$

Eq. (11) is the weak form of the total form sensitivity equation. Since virtual displacement \bar{w} is arbitrary, it can be chosen as $\bar{w}(X + bV(X)) = \bar{w}(X)$. That is \bar{w} can be chosen as constant along $X_b = X + bV(x)$, so that

$$\dot{\bar{w}} = 0 \quad (12)$$

Even if it is assumed that $\dot{\bar{w}} \neq 0$, since \bar{w} is in the space of kinematically admissible virtual displacements, it satisfies the weak form relation.¹³

The CSE method is especially efficient for nonlinear problems, since the CSE is always linear. If iterative Newton-Raphson's method is used for solving the nonlinear analysis problem associated with a Galerkin finite element method, the tangent stiffness matrix of the last iteration gives the required matrix to solve the linear CSE as will see in the following sections. Wickert states⁵ that although this applies to the Galerkin method, it is not generally true for other weighted-residual forms such as the Least Square finite element methods.

The CSE method in local derivative form uses only the analysis solution on the boundary, but the finite element approximation of derivatives of the solution may not be accurate enough on the boundary.²⁰ In contrast, the total derivative form CSE requires information from the analysis solution in the domain, where the finite element solution may be more accurate. Higher order derivatives of the analysis solution at boundaries are needed for local derivative form, which are less accurate, when they are obtained by differentiating of the solution.²¹ Moreover, when the solution contains a strain discontinuity, the local sensitivity variable is not continuous. Then a special treatment is needed to handle discontinuous local sensitivity variables at joints.⁶ For the total derivative form CSE using domain integration, the fact that the total sensitivity at joined points is continuous greatly simplifies the implementation. The sensitivity coefficient matrix for the discretized CSE is assembled based on the continuity of the total sensitivity variables. This attribute makes the total derivative form more practical for built-up structures.

To summarize, the CSE system is a linear boundary value problem derived by taking the derivatives of the original field equations, Eq. (1) and boundary conditions, Eq. (2). The continuum sensitivity equations may be derived in either total or local derivative form. When expressed in local form, only the boundary parameterization needs to be described. In total derivative form, the parameterization or transformation function for the entire domain is necessary, which is equivalent to the mesh Jacobian after discretization. Posing the CSE in local derivative form and parameterizing the boundary as described above avoids the numerical complexity and expense of the domain transformation and mesh Jacobian. Next we will illustrate how to derive the total derivative form sensitivity equations for particular examples.

III. Transient joined beam with an airfoil under gust load model

A joined-beam structure is modeled as a NACA0012 airfoil mounted on a sting with a supporting strut. This simple two-dimensional model in Fig. 1 has features representative of a three-dimensional joined wing. The three-beam model represents a two-dimensional analog to large spanwise deflection and buckling of the aft wing. The sting and strut are modeled as nonlinear Timoshenko beams capable of large deflections. At a positive angle of attack, the airfoil generates lift, deflecting the beam in the fluid, resulting in an increased angle of attack. Equilibrium deflection of the sting occurs when the force and moments generated by the lifting airfoil balance the internal sting force and moments resisting the bending. The strut is subject to a buckling load due to the deflection of the sting. The buckling load arises from aerodynamic forces calculated from solving potential flow around the airfoil. For shape sensitivity analysis, the sting length L is taken as shape design parameter.

A. Timoshenko beam governing equations and weak forms

Nonlinear Timoshenko beam theory accounts for large rotations but with small strains.²² The displacement field can be given as

$$u_x = u(x) - z\psi, \quad u_y = 0, \quad u_z = w(x)$$

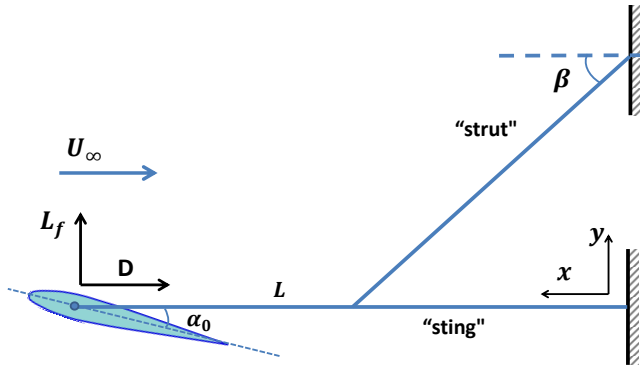


Figure 1. Joined beam with an airfoil model.

where ψ is the rotation of the cross section. Using the nonlinear strain-displacement relations

$$\epsilon_{ij} = \frac{1}{2}(u_{i,j} + u_{j,i}) + \frac{1}{2}(u_{m,i}u_{m,j})$$

and omitting the large strain terms but retaining only the square of rotation of a transverse normal line in the beam, we obtain

$$\epsilon_{xx} = \left[\frac{\partial u}{\partial x} + \frac{1}{2} \left(\frac{\partial w}{\partial x} \right)^2 \right] - z \frac{\partial \psi}{\partial x}; \quad \gamma_{xz} = \frac{\partial w}{\partial x} - \psi$$

By using extended Hamilton's principle, the governing equations for the nonlinear Timoshenko beam with the rotational inertia can be derived as

$$\rho A u_{,tt} - \left[EA(u_{,x} + \frac{1}{2} w_{,x}^2) \right]_{,x} - f = 0 \quad (13)$$

$$\rho A w_{,tt} - \left[EA w_{,x} (u_{,x} + \frac{1}{2} w_{,x}^2) \right]_{,x} - [kGA(w_{,x} - \psi)]_{,x} - q = 0 \quad (14)$$

$$\rho I \psi_{,tt} - (EI \psi_{,x})_{,x} - kGA(w_{,x} - \psi) = 0 \quad (15)$$

where w is the vertical deflection, u is the axial displacement, ψ is the rotation angle to the y axis, f is axially distributed load and q is the laterally distributed load. The weak form of the nonlinear Timoshenko beam model is

$$\int_{x_a}^{x_b} \rho A u_{,tt} v_1 dx + \int_{x_a}^{x_b} EA(u_{,x} + \frac{1}{2} w_{,x}^2) v_{1,x} dx = \int_{x_a}^{x_b} v_1 f dx + N_{xx} v_1|_{x_a}^{x_b} \quad (16)$$

$$\int_{x_a}^{x_b} \rho A w_{,tt} v_2 dx + \int_{x_a}^{x_b} EA w_{,x} (u_{,x} + \frac{1}{2} w_{,x}^2) v_{2,x} dx + \int_{x_a}^{x_b} kGA(w_{,x} - \psi) v_{2,x} dx = \int_{x_a}^{x_b} v_2 q dx + V_f v_2|_{x_a}^{x_b} \quad (17)$$

$$\int_{x_a}^{x_b} \rho I \psi_{,tt} v_3 dx + \int_{x_a}^{x_b} EI \psi_{,x} v_{3,x} dx - \int_{x_a}^{x_b} kGA(w_{,x} - \psi) v_3 dx = M_{xx} v_3|_{x_a}^{x_b} \quad (18)$$

We have the axial force N_{xx} , moment on cross section M_{xx} , shear force on cross section Q_x and the vertical force V_f as listed below

$$\begin{aligned} N_{xx} &= EA(u_{,x} + \frac{1}{2} w_{,x}^2); \quad M_{xx} = EI \psi_{,x} \\ Q_x &= -kGA(w_{,x} - \psi); \quad V_f = N_{xx} W_{,x} - Q_x \end{aligned}$$

B. Total derivative form CSE

For deriving the CSE,¹³ firstly, we write the first weak form Eq. (16) as

$$\int_{x_a}^{x_b} C(u, w, v_1) dx - N_{xx} v_1|_{x_a}^{x_b} = 0 \quad (19)$$

where $C(u, w, v_1)$ is the integrand of the weak form of Eq.(16). Taking total derivative of the weak form (19) with respect the design variable by using Eq. (9) and Eq. (10), we have

$$\int_{x_a}^{x_b} C'(u, w, v_1) + \operatorname{div} [C(u, w, v_1)V(x)] dx = \dot{N}_{xx} v_1|_{x_a}^{x_b} \quad (20)$$

Substituting the integrand of (16) into (20) and carrying out the derivatives, we have

$$\begin{aligned} 0 = \int_{x_a}^{x_b} & \rho A \dot{u}_{,tt} v_1 + \rho A \dot{u}_{,tt} v_1 V_{,x} + [EA(u'_{,x} + w_{,x} w'_{,x})] v_{1,x} + EA[u_{,x} + \frac{1}{2} w_{,x}^2] v'_{1,x} - v'_1 f - v_1 f' \\ & V \left[EA(u_{,xx} + w_{,x} w_{,xx}) v_{1,x} + EA[u_{,x} + \frac{1}{2} w_{,x}^2] v_{1,xx} - v_{1,x} f - v_1 f_{,x} \right] + \\ & V_{,x} \left[EA(u_{,x} + \frac{1}{2} w_{,x}^2) v_{1,x} - v_1 f \right] dx - \dot{N}_{xx} v_1|_{x_a}^{x_b} \end{aligned} \quad (21)$$

where

$$\begin{aligned} u'_{,x} &= \dot{u}_{,x} - u_{,xx} V - u_{,x} V_{,x} \\ w'_{,x} &= \dot{w}_{,x} - w_{,xx} V - w_{,x} V_{,x} \\ v'_{1,x} &= \dot{v}_{1,x} - v_{1,xx} V - v_{1,x} V_{,x} \end{aligned} \quad (22)$$

Simplifying equation (21) by using the partial derivatives in Eq. (22) and Eq. (12), we obtain the weak form of the CSE for Eq. (16) as

$$\begin{aligned} \int_{x_a}^{x_b} & \rho A \dot{u}_{,tt} v_1 dx + \int_{x_a}^{x_b} EA [\dot{u}_{,x} + \dot{w}_{,x} w_{,x}] v_{1,x} - v_1 \dot{f} dx = \\ & \int_{x_a}^{x_b} [EA(u_{,x} + w_{,x}^2) v_{1,x} + v_1 f] V_{,x} dx - \int_{x_a}^{x_b} \rho A u_{,tt} v_1 V_{,x} dx + \dot{N}_{xx} v_1|_{x_a}^{x_b} \end{aligned} \quad (23)$$

Similarly, we can get the CSE weak form of Eq. (17) and Eq. (18) as

$$\begin{aligned} \int_{x_a}^{x_b} & \rho A \dot{w}_{,tt} v_2 dx + \int_{x_a}^{x_b} \left[EA \dot{w}_{,x} (u_{,x} + \frac{1}{2} w_{,x}^2) + EA w_{,x} (\dot{u}_{,x} + w_{,x} \dot{w}_{,x}) + kGA(\dot{w}_{,x} - \dot{\psi}) \right] v_{2,x} - \dot{q} v_2 dx = \\ & \int_{x_a}^{x_b} \left[\left(EA w_{,x} (2u_{,x} + \frac{3}{2} w_{,x}^2) + kGA w_{,x} \right) v_{2,x} + q v_2 \right] V_{,x} dx - \int_{x_a}^{x_b} \rho A w_{,tt} v_2 V_{,x} dx + \dot{V}_f v_2|_{x_a}^{x_b} \end{aligned} \quad (24)$$

$$\int_{x_a}^{x_b} \rho I \dot{\psi}_{,tt} v_3 + EI \dot{\psi}_{,x} v_{3,x} - kGA(\dot{w}_{,x} - \dot{\psi}) v_3 dx = \int_{x_a}^{x_b} (EI \dot{\psi}_{,x} v_{3,x} - kGA \psi v_3 - \rho I \dot{\psi}_{,tt} v_3) V_{,x} dx + \dot{M}_{xx} v_3|_{x_a}^{x_b} \quad (25)$$

Equations (23)-(25) are the weak form of the CSE equations in the total derivative form. The right hand side of the equations are explicitly dependent on the design velocity $V(x)$ and the analysis solution. The total discrete sensitivity can be obtained by solving this set of equations for the total sensitivity variables using the same method for solving the analysis problem. In contrast to the local derivative form, only first order derivatives of the analysis solution are required, but the design velocity and its derivative is needed throughout the domain when domain integration method is used.

C. Aerodynamic model around airfoil

The flow around the airfoil is model as linear potential flow, which is used to demonstrate the application of continuum sensitivity method to the two dimension flow problems. In an irrotational flow, the governing equation for the stream function Ψ is

$$\nabla^2 \Psi = 0 \quad (26)$$

The x and y-component velocity, v_x and v_y , can be found from the streamfunction, Ψ , in two dimensional flows,

$$v_x = \frac{\partial \Psi}{\partial y}, \quad v_y = -\frac{\partial \Psi}{\partial x} \quad (27)$$

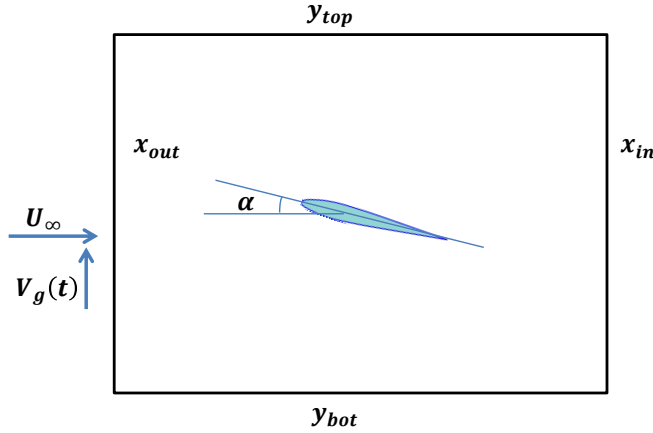


Figure 2. Potential Flow Around an Airfoil model.

At the left and right of the computational domain as seen in Fig. 2, the natural boundary condition is

$$F = n_x \frac{\partial \Psi}{\partial x} + n_y \frac{\partial \Psi}{\partial y} \quad (28)$$

where n_x and n_y is the x and y direction components of the boundary normal vector \vec{n} . If the inflow velocity magnitude is U_∞ with an angle of attack α , the flux on the left and right boundary, F_l and F_r are given as

$$F_l = V_g(t), \quad F_r = -V_g(t) \quad (29)$$

the essential boundary conditions on the top and bottom boundary of the domain are given as

$$\Psi = U_\infty y - V_g(t)x \quad (30)$$

The wall boundary condition on the airfoil is the no-penetration condition. If airfoil boundary is a streamline then the velocity always tangential to the airfoil. Thus, the no-penetration condition becomes an essential boundary condition on the airfoil, which is

$$\Psi|_{\Gamma_a} = \Psi_a \quad (31)$$

where Ψ_a is a constant along the airfoil but it's not known prior to the simulation. The Kutta condition was used as another constraint. It requires the flow to leave the trailing edge smoothly. To enforce this condition, we require that flow at the trailing edge be aligned along the bisector of the trailing edge, \hat{t}_{TE} . The geometry of the trailing edge is shown in Fig. 3. For the flow to be aligned to \hat{t}_{TE} , the velocity normal to the bisector \hat{t}_{TE} should be zero. Thus, at the trailing edge, the Kutta condition becomes,

$$\nabla \Psi \cdot \hat{t}_{TE} = 0 \quad (32)$$

The finite element method is used for solving the analysis problem. The weak form of Eq. (26) is

$$\iint_{\Omega} \nabla \bar{w} \cdot \nabla \Psi dA = \oint_{\Gamma} \bar{w} q_n ds \quad (33)$$

where \bar{w} is the test function, Ω is the fluid domain, Γ is the boundary of the domain and $q_n = \frac{\partial \Psi}{\partial x} n_x + \frac{\partial \Psi}{\partial y} n_y$ is the flux through the boundaries.

The vertical gust is modeled using the usual discrete gust idealization of a one-minus-cosine pulse,²³ so that

$$V_g(t) = \begin{cases} \frac{1}{2} V_{g,max} \left(1 - \cos \frac{t - \tau_0}{T_g} \right) & \tau_0 \leq t \leq T_g \\ 0 & o \cdot w. \end{cases} \quad (34)$$

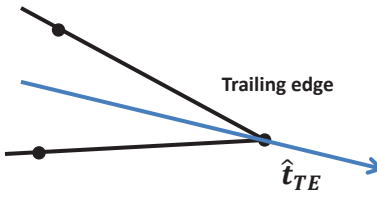


Figure 3. Trailing Edge Geometry.

where $V_{g,max}$ is the maximum amplitude of the gust, τ_0 is the start of the gust, and T_g is the duration of the gust. Since the NACA0012 is symmetric and the tip of the sting is mounted at the aerodynamic center of the airfoil, the aerodynamic moment is zero.

D. Total form CSE for fluid domain

For total form CSE, the weak form of the governing equation (33) is differentiated by using the equations (9) and (10) for material derivatives in section II. We obtain the weak form of the CSE system in terms of the total sensitivity variable $\dot{\Psi}$ as

$$\iint_{\Omega} \nabla \dot{\Psi} \cdot \nabla \bar{w} dA = \iint_{\Omega} \left((\nabla V)^T \nabla \bar{w} \right) \cdot \nabla \dot{\Psi} + \nabla \bar{w} \cdot \left((\nabla V)^T \nabla \dot{\Psi} \right) + (\nabla \bar{w} \cdot \nabla \dot{\Psi}) (\nabla \cdot V) dA \quad (35)$$

The material derivative of the boundary term vanishes, since the boundary integral is constant at far field boundary. The CSE boundary constraint for the Kutta condition can be derived by taking the total derivative of Eq. (32) and moving the convective terms to the right hand side as

$$\nabla \dot{\Psi} \cdot \hat{t}_{TE} = (\nabla V)^T \nabla \dot{\Psi} - \nabla \dot{\Psi} \cdot \frac{D \hat{t}_{TE}}{D b} \quad (36)$$

The CSE boundary conditions on the outer boundary of the domain are the same as the boundary condition for the local form CSE system, since the nodes on these boundaries do not change with the shape design variables. The essential boundary conditions on the airfoil can be derived by take total derivative of Eq. (31).

$$\dot{\Psi}|_{\Gamma_a} = \dot{\Psi}_a \quad (37)$$

Equation (37) has the same form of the essential boundary condition of the original analysis problem. The way we implement this condition is the same as solving the analysis problem. The variable $\dot{\Psi}_a$ is treated as an unknown to be found for all nodes on the airfoil in the same way as for analysis problem.

The material derivative of the flow velocity can be obtained by taking the total derivative of Eq. (27) as

$$\dot{u} = -\dot{\Psi}_{,x} + \nabla \dot{\Psi} \cdot V_{,x} \quad (38)$$

$$\dot{v} = \dot{\Psi}_{,y} - \nabla \dot{\Psi} \cdot V_{,y} \quad (39)$$

where $V_{,x}$ and $V_{,y}$ are the spatial derivatives of the design velocity. The pressure coefficient in an inviscid, incompressible flow can be obtained using Bernoulli's equation.

$$C_p = \frac{p - p_{\infty}}{\frac{1}{2} \rho_a U_{\infty}^2} = 1 - \left(\frac{\bar{v}}{U_{\infty}} \right)^2 \quad (40)$$

where $\bar{v} = \sqrt{v_x^2 + v_y^2}$ is the local flow speed. Hence the material derivative of the pressure coefficient is

$$\dot{C}_p = \frac{2(u\dot{u} + v\dot{v})}{U_{\infty}^2} \quad (41)$$

The total sensitivity of the stream function $\dot{\Psi}$ can be obtained by solving the total form CSE (35). It requires only first derivative of the dependent variable Ψ throughout the domain, while second derivative of the stream function is required by local form CSE on the boundary.²¹ The accuracy of the sensitivity of the pressure coefficient by total form CSE is not degraded as for the local form CSE, since the second spatial derivatives of the flow variables are not needed. Therefore, the total form CSE may be more accurate than the local form CSE, especially at the flow field boundaries where the finite element method tends to give less accurate results for the derivatives.

The boundary design velocity field can be obtained directly from the relation between the boundary geometry and the shape parameters. Given the design velocity on the boundary \bar{V} as required by the local form CSE, a pseudo solid method may be used for calculating the design velocity inside the domain.²⁴ In this method, the domain design velocity is governed by the linear equations of elasticity.

$$\nabla \cdot \boldsymbol{\sigma} + \mathbf{f} = 0 \quad (42)$$

where \mathbf{f} is the prescribed body force, which is zero here. The stress $\boldsymbol{\sigma}$ is related to the strain tensor as

$$\boldsymbol{\sigma} = \lambda(\text{tr } \boldsymbol{\epsilon})\mathbf{I} + 2\mu\boldsymbol{\epsilon} \quad (43)$$

where \mathbf{I} is the identity matrix, λ and μ are the so-called *Lamé* constants, which are related to the commonly used Young's modulus E and poisson's ratio ν as

$$\mu = \frac{E}{2(1 + \nu)} \quad (44)$$

$$\lambda = \frac{E\nu}{(1 + \nu)(1 - 2\nu)} \quad (45)$$

The strain tensor is related to the design velocity gradients by the expression

$$\boldsymbol{\epsilon} = \frac{1}{2} (\nabla V + (\nabla V)^T) \quad (46)$$

The Dirichlet boundary condition for the pseudo-solid is imposed by the design velocity on the boundary, and represented by

$$V(x) = \bar{V}(x) \text{ on } \Gamma \quad (47)$$

Solving the linear elasticity equations, the design velocity throughout the domain can be obtained, and the design velocity field satisfies the linear dependency requirements, which requires that the design velocity field in the domain should depend linearly on the variation of the shape design variable.¹ The design velocity field should be compatible with the mesh updating in shape optimization. For avoiding the large mesh distortion, it is desirable to preserve the element shape in fine mesh areas, and make the larger elements deform more than the smaller elements. Also to avoid large strain in sharp corners, which is the required spatial derivative of the design velocity, the elements at those corners are weighted to have large stiffness. This can be implemented by refining the mesh at sharp corners and by replacing the Jacobian of the transformation between the physical and the computational domain with its reciprocal or just by dropping the Jacobian.²⁴

The pseudo solid method can also be used for the mesh movement of the fluid-structure interaction solver. Exactly the same pseudo solid governing equations and numerical method can be adopt with different values for the essential boundary condition in (47). Hence, the factorized stiffness matrix for mesh moving can be saved and reused for calculating the design velocity field inside the domain, which saves computational time.

IV. Results

A joined beam with an airfoil model serves an example for verification of the CSE method for transient aeroelasticity problems. As seen in Fig. 1, the joined beam deforms under the aerodynamic force while the tip rotation increases the angle of attack of the airfoil, and then further increases the aerodynamic forces. This flow model is actually a quasi-steady flow, since the inertia and elastic effect of the flow are not considered. A loosely coupled algorithm is adopted for solving the aeroelastic system. The fluid mesh moves according to the deformation of the sting. A mesh moving algorithm based on pseudo solid method has been implemented. By adjusting the Young's modulus and the poisson's ratio, this algorithm can deal with fairly

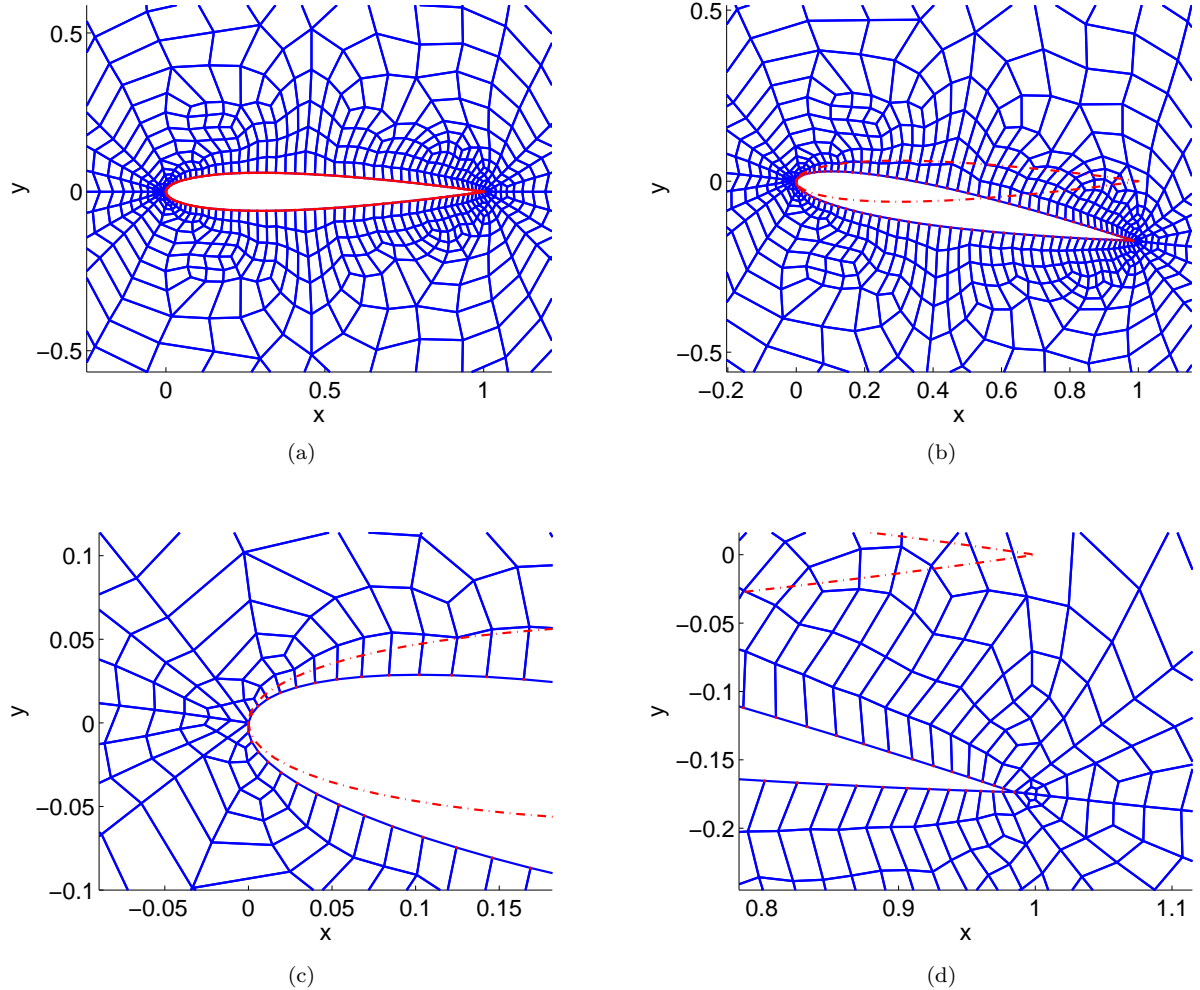


Figure 4. Mesh movement for airfoil deformation, (a) original mesh, (b) deformed mesh, (c) zoom in at leading edge (d) zoom in at trailing edge

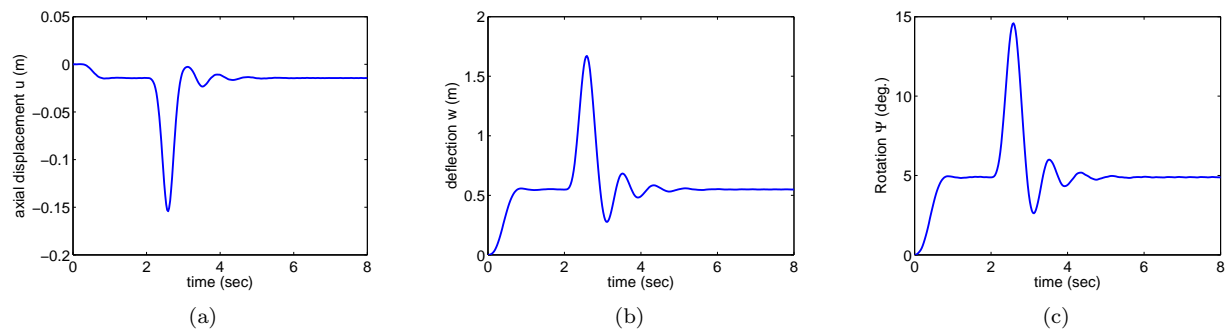


Figure 5. Joined beam gust response at sting tip

large mesh deflection. As shown in Fig. 4, as a test case, the mesh movement due to airfoil rotation was calculated. The subfigure (a) is the original fluid mesh for flow around a NACA0012 airfoil. By specifying the shape deformation at the airfoil boundary, the nodes of the mesh move according to the pseudo solid deformation. As can be seen in subfigure (c) and (d), the mesh quality is good at the leading and trailing edge although the deformation is fairly large. This pseudo solid method has also been used for calculating

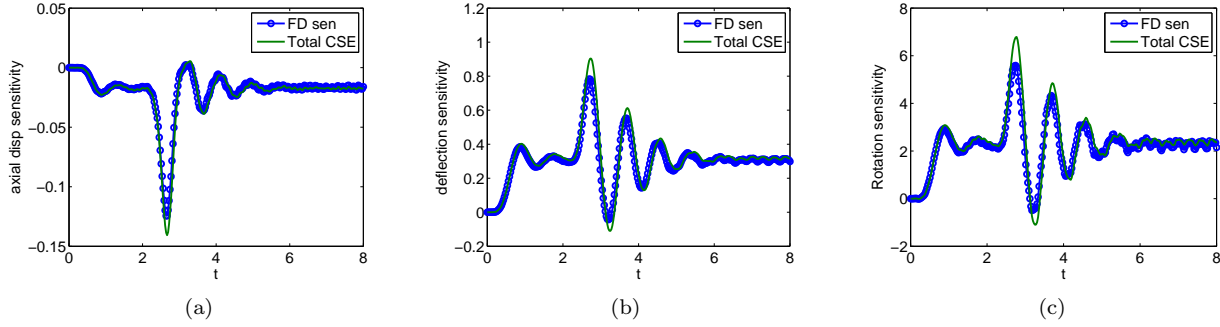


Figure 6. Joined beam tip gust response sensitivity w.r.t beam length

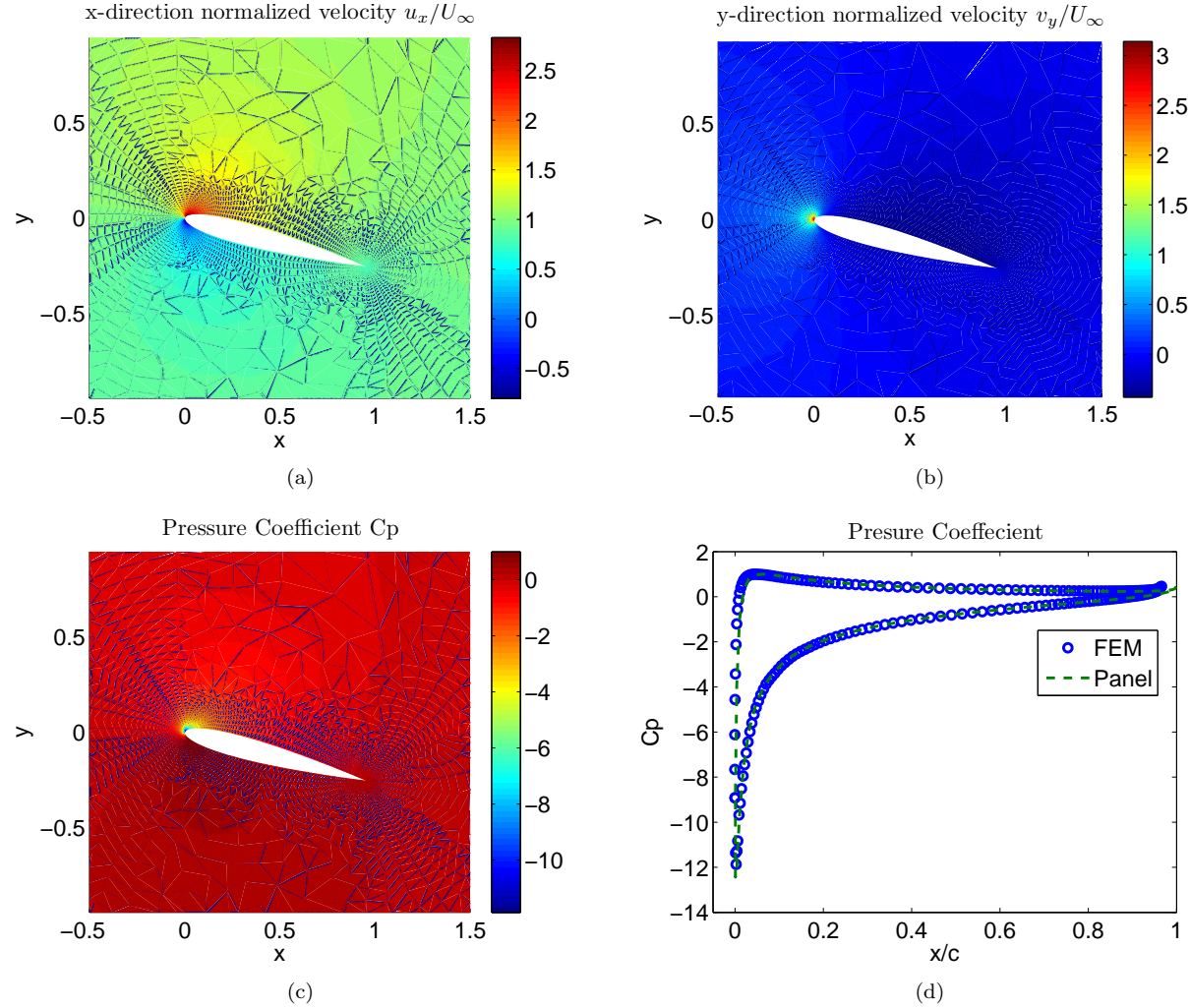


Figure 7. Finite element solutions for flow around airfoil at $t = 2.65s$

the design velocity field inside the domain for total form CSE method.²¹

The transient gust response was investigated and the FSI responses at the sting tip are plotted in Fig. 5. Before the gust arrives at $t = 2s$, the joined beam structure reached steady state. When the gust arrives, the structure has a large deflection, and the nonlinear model captures the shortening effects as seen in subfigure (a). After the gust leaves at $t = 3$, the vibration is damped out due to the aerodynamic damping and the response goes back to state steady. Inside each nonlinear iteration loop for the structure of each time

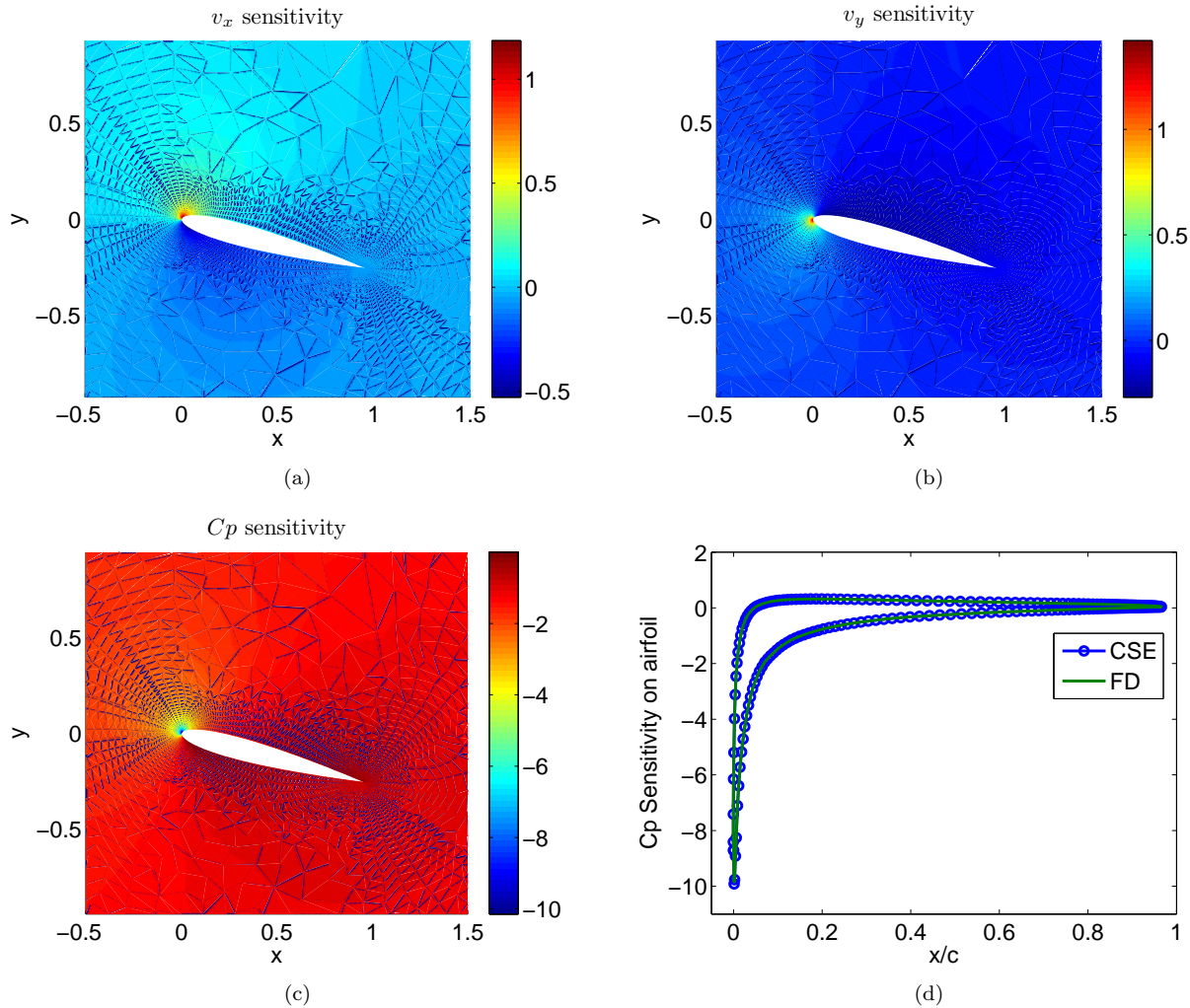


Figure 8. Sensitivity of flow velocity and pressure with respect to beam length at $t = 2.65s$.

point, a quasi-steady potential flow is solved to obtain the aerodynamic force exerted on the sting. The flow solutions around the airfoil of the last iteration of the nonlinear solver at $t = 2.65$ (when the response has the maximum magnitude) are plotted in Fig. 7. The velocity in x direction in subfigure (a) increases on the upper airfoil surface and decreases on the lower airfoil surface. The velocity in y direction increases rapidly at the upper leading edge. Hence, the pressure coefficient has positive values at the upper leading edge and has negative values at the lower leading edge. As seen in subfigure (d), the pressure coefficient around the airfoil closely matches a vortex panel code solution.²⁵

The transient gust response sensitivities with respect to the sting length are calculated by using the total derivative form CSE method. The total form derivative was easier to implement than the local form, since no special treatment is needed at the joint node. As can be seen in Fig. 6, the nonlinear joined beam gust response sensitivity by total form CSE method matches the finite difference results with small accuracy difference at the peaks of the response. In each time step, the pressure sensitivity on the airfoil with respect to the sting length are calculated, then the pressure sensitivity are integrated to obtain the lift sensitivity that required by the CSE system for structure. The flow sensitivities at time $t = 2.65$ are shown in Fig. 8. At time $t = 2.65$, when the length of the sting increases, the rotation of the tip of the sting increases, hence the angle of attack increases accordingly. As a result, the velocities at the upper airfoil surface increase and the velocities at the lower airfoil surface decrease. Hence, the velocity sensitivities shown in Fig. 8 are positive on the upper surface and negative on the lower surface, while the pressure coefficient sensitivity is negative on the upper surface and positive on the lower surface. As seen from subfigure(d), the pressure coefficient

sensitivity on the airfoil surface closely matches the finite difference solution.

V. Conclusions

In this paper, a fluid-structure interaction solver is developed and applied to a joined beam with an airfoil under transient gust load. The pseudo solid method is implemented for both mesh movement and the design velocity calculation. The factorized stiffness matrix for mesh movement can be used for design velocity field calculation. The CSE method in total form is developed for shape design sensitivity analysis. The shape sensitivity results for transient nonlinear joined beam under a quasi-steady potential flow are obtained and compared well with finite difference results. The flow sensitivity in this paper is a shape design problem, whereas it was a value design problem in the previous publications by author of this paper. Because the fluid domain deforms with the design here rather than rotates rigidly with the structural deformation.

The CSE method can either be derived in local form or in total form. The advantage of local form CSE method is that it requires only design velocity at the boundaries of the field, while the total form CSE requires a design velocity field throughout the domain. Calculating the design velocity field often involves solving a linear system of equations. The local sensitivity variables in the CSE system are not continuous at a joint or other structural interfaces with strain discontinuities. Hence, the elemental sensitivity matrix cannot be assembled directly based on the continuity of the dependent variables. A special treatment should be implemented at each joint node as shown by Liu and Canfield.⁶ The total derivative form CSE is more applicable for built-up structures, since no special treatment of the interface conditions is required as for the local form.

VI. Acknowledgements

This material is based on research sponsored by Air Force Office of Scientific Research under agreement number FA9550-09-1-0354. The authors gratefully acknowledge the support of AFOSR program manager Dr. Fariba Fahroo and the AFRL Senior Aerospace Engineers Dr. Raymond Kolonay, Dr. Phillip Beran, and Dr. Maxwell Blair.

References

- ¹Haug, E. J., Choi, K. K., and Komkov, V., *Design sensitivity analysis of structural systems, Mathematics in science and engineering.*, Vol. 177, Academic Press, Orlando, 1986.
- ²Borggaard, J. and Burns, J., "A PDE Sensitivity Equation Method for Optimal Aerodynamic Design." *Journal of Computational Physics.*, Vol. 136, 1997, pp. 366–384.
- ³Haftka, R. T. and Gurdal, Z., *Design sensitivity analysis of structural systems, Mathematics in science and engineering.*, Vol. 177, Academic Press, Orlando, 1986.
- ⁴Borggaard, J. and Burns, J., "A Sensitivity Equation Approach to Shape Optimization in Fluid Flows." Tech. rep., Langley Research Center, 1994.
- ⁵Wickert, D. P., *Least-Squares, Continuous Sensitivity Analysis for Nonlinear Fluid-structure Interaction Problems.*, Ph.D. thesis, Air Force Institute of Technology, Ohio, aug 2009.
- ⁶Liu, S. and Canfield, R. A., "Continuum Shape Sensitivity for Nonlinear Transient Aeroelastic Gust Response." *52nd AIAA/ASME/ASCE/AHS/ASC Structures, Structural Dynamics, and Materials Conference*, No. AIAA 2011-1971, Denver, Colorado, April, 4-7 2011.
- ⁷Dems, K. and Haftka, R. T., "Two Approaches to Sensitivity Analysis for Shape Variation of Structures." *Mech. Struct.& Mach.*, Vol. 16, No. 4, 1988-1989, pp. 501.
- ⁸Dems, K. and Mroz, Z., "Variational approach to first- and second-order sensitivity analysis of elastic structures." *International Journal for Numerical Methods in Engineering*, Vol. 21, 1985, pp. 637–661.
- ⁹Jameson, A., "Aerodynamic design via control theory," *Journal of Scientific Computing*, Vol. 3, 1988, pp. 233–260, 10.1007/BF01061285.
- ¹⁰Bhaskaran, R. and Berkooz, G., "Optimization of Fluid-Structure Interaction using the Sensitivity Equation Approach." *Fluid-Structure Interaction, Aeroelasticity, Flow-Induced Vibrations and Noise.*, Vol. 1, No. 53-1, 1997, pp. 49–56.
- ¹¹Turgeon, E., Pelletier, D., and Borggaard, J., "A Continuous Sensitivity Equation Approach to Optimal Design in Mixed Convection." No. AIAA 99-3625, 1999.
- ¹²Stanley, L. G. D. and Stewart, D., *Design sensitivity analysis : computational issues of sensitivity equation methods.*, Academic Press, Philadelphia, 2002.
- ¹³Choi, K. K. and Kim, N.-H., *Structural sensitivity analysis and optimization.*, Springer Science+Business media, New York, 2005.
- ¹⁴Etienne, S. and Pelletier, D., "A general approach to sensitivity analysis of fluid-structure interactions." *Journal of Fluids and Structures*, Vol. 21, No. 2, 2005, pp. 169–186.

¹⁵Etienne, S., Hay, A., and Garon, A., "Shape Sensitivity Analysis of Fluid-Structure Interaction Problems." No. AIAA 2006-3217, 2006.

¹⁶Etienne, S., Hay, A., and Garon, A., "Sensitivity Analysis of Unsteady Fluid-Structure Interaction Problems." No. AIAA-2007-332, 2007.

¹⁷Wickert, D. P., Canfield, R. A., and Reddy, J. N., "Fluid-Structure Transient Gust Sensitivity Using Least-Squares Continuous Sensitivity Analysis." *50th AIAA/ASME/ASCE/AHS/ASC Structures, Structural Dynamics, and Materials Conference*, No. AIAA-2008-1821, Palm Springs, California, May 4-7 2009.

¹⁸Liu, S., Wickert, D. P., and Canfield, R. A., "Fluid-Structure Transient Gust Response Sensitivity for a Nonlinear Joined Wing Model." *51st AIAA/ASME/ASCE/AHS/ASC Structures, Structural Dynamics, and Materials Conference*, Orlando, Florida, April, 12-15), Number=AIAA 2010-3118 2010.

¹⁹Dems, K. and Mroz, Z., "Variational approach by means of adjoint systems to structural optimization and sensitivity analysis. I - Variation of material parameters within fixed domain." *International Journal of Solids and Structures*, Vol. 19, No. 8, 1983, pp. 677-692.

²⁰Yang, R. J. and Botkin, M. E., "The relationship between the variational approach and the implicit differentiation approach to shape design sensitivities." *Bennett JA, Botkin ME (eds) The optimum shape: automated structural design. Plenum, New York*, 1986, pp. 61-77.

²¹Liu, S. and Canfield, R. A., "Continuum Shape Sensitivity Method for Fluid Flow Around an Airfoil." *53st AIAA/ASME/ASCE/AHS/ASC Structures, Structural Dynamics, and Materials Conference*, No. AIAA 2012-1426, Honolulu, Hawaii, April, 23-26 2012.

²²Reddy, J. N., *An introduction to nonlinear finite element analysis.*, McGraw-Hill series in mechanical engineering, McGraw-Hill Higher Education, New York, NY, 2006.

²³Hoblit, F. M., *Gust loads on aircraft : concepts and applications.*, AIAA education series, American Institute of Aeronautics and Astronautics., Washington, D.C., 1988.

²⁴Johnson, A. A. and Tezduyar, T. E., "Mesh update strategies in parallel finite element computations of flow problems with moving boundaries and interfaces," *Computer Methods in Applied Mechanics and Engineering*, Vol. 119, 1994, pp. 73-94.

²⁵Marchman, J. F., "PANEL: A "Smith-Hess" type of 2-D panel code combining source panels and vortices for a single-element, lifting airfoil in incompressible flow," Virginia Tech, 1999.